Article

Chinese Science Bulletin

SPECIAL ISSUE: Extreme Climate in China

April 2013 Vol.58 No.12: 1427–1435
doi: 10.1007/s11434-012-5533-0

East Asian monsoon change for the 21st century: Results of CMIP3 and CMIP5 models

JIANG DaBang[1,2,3*] & TIAN ZhiPing[1,4]

[1] *Nansen-Zhu International Research Centre, Institute of Atmospheric Physics, Chinese Academy of Sciences, Beijing 100029, China;*
[2] *Key Laboratory of Regional Climate-Environment Research for Temperate East Asia, Chinese Academy of Sciences, Beijing 100029, China;*
[3] *Climate Change Research Center, Chinese Academy of Sciences, Beijing 100029, China;*
[4] *University of Chinese Academy of Sciences, Beijing 100049, China*

Received July 1, 2012; accepted September 28, 2012; published online November 30, 2012

Forty-two climate models participating in the Coupled Model Intercomparison Project Phases 3 and 5 were first evaluated in terms of their ability to simulate the present climatology of the East Asian winter (December–February) and summer (June–August) monsoons. The East Asian winter and summer monsoon changes over the 21st century were then projected using the results of 31 and 29 reliable climate models under the Special Report on Emissions Scenarios (SRES) mid-range A1B scenario or the Representative Concentration Pathways (RCP) mid-low-range RCP4.5 scenario, respectively. Results showed that the East Asian winter monsoon changes little over time as a whole relative to the reference period 1980–1999. Regionally, it weakens (strengthens) north (south) of about 25°N in East Asia, which results from atmospheric circulation changes over the western North Pacific and Northeast Asia owing to the weakening and northward shift of the Aleutian Low, and from decreased north-west-southeast thermal and sea level pressure differences across Northeast Asia. In summer, monsoon strengthens slightly in East China over the 21st century as a consequence of an increased land-sea thermal contrast between the East Asian continent and the adjacent western North Pacific and South China Sea.

global warming, East Asian monsoon, climate models, projection

Citation: Jiang D B, Tian Z P. East Asian monsoon change for the 21st century: Results of CMIP3 and CMIP5 models. Chin Sci Bull, 2013, 58: 1427–1435, doi: 10.1007/ s11434-012-5533-0

The East Asian monsoon has varied over a range of time-scales since the mid-20th century. Among these include a weakened trend from the mid-1960s and a slight recovery from the early 1990s for the East Asian summer (June–August) monsoon (EASM), a weakened trend of the East Asian winter (December–February) monsoon (EAWM) since the mid-late 1980s, and a changed relationship between the East Asian monsoon and global climate [1–11]. Because change in the East Asian monsoon is directly related to climate anomalies such as floods and droughts in East China, and hence impacts greatly on the national economy and people's daily lives, how it might change under future global warming is one of the central issues in climate change research. In recent years, more and more attention has been paid to the projection of climate change in China. However, most of this has focused on temperature, precipitation, and their extremes. Little emphasis has been placed upon the East Asian atmospheric circulation, including the East Asian monsoon [7,12,13].

In theory, the rate of surface temperature increase is stronger over land than over the oceans in the process of global warming, and monsoon should strengthen accordingly in response to an increased land-sea thermal contrast. However, this hypothesis does not consider the interaction of changes in large-scale atmospheric circulations, and whether it is effective for the complicated East Asian monsoon system [14,15] remains unclear. In the literature, opinion differs on the response of the East Asian monsoon

*Corresponding author (email: jiangdb@mail.iap.ac.cn)

to increased atmospheric greenhouse gas concentrations based on numerical experiments of either individual or multiple climate models. Among those opinions, the EASM is projected to strengthen [5,7,16–19], strengthen slightly only over South China [20,21], vary little [22], and remain normal in terms of intensity [23]; while the EAWM is projected to weaken [7,16,24], weaken over East China [25], weaken slightly over East China [17], and strengthen only over Northeast China [22]. Given that there are differences in climate models, emissions scenarios, and analysis methods among those studies, and that most of them do not assess whether climate models can reliably reproduce the present East Asian monsoon circulation, it is difficult to obtain a consistent view of the future East Asian monsoon. At present, the focus is to use the outputs of reliable climate models to project future changes in the East Asian monsoon from the perspective of multiple climate models and climate dynamics, particularly based on state-of-the-art climate models worldwide.

Taken together, using all available data of climate models participating in the Intergovernmental Panel on Climate Change (IPCC) Assessment Reports Four and Five, this study assesses the changes in the EASM and EAWM over the 21st century under the Special Report on Emissions Scenarios (SRES) mid-range A1B scenario or the Representative Concentration Pathways (RCP) mid-low-range RCP4.5 scenario. Particular emphasis is given to the most common changes among climate models and the underlying dynamical mechanisms.

1 Data and methods

Many climate models have been used to simulate the present and future climates in the Coupled Model Intercomparison Project Phases 3 (CMIP3) and 5 (CMIP5). According to the availability of output data from the CMIP3 20th Century Climate in Coupled Models (20C3M) simulation, the CMIP5 historical simulation, the CMIP3 SRES A1B [26] simulation, and the CMIP5 RCP4.5 [27,28] simulation, the results of 23 and 19 climate models archived respectively in the CMIP3 and CMIP5 were applied in the present study. Basic information about those climate models and experiments is provided in Table 1. More details are available online at http://www-pcmdi.llnl.gov/ipcc/about_ipcc.php and http://cmip-pcmdi.llnl.gov/cmip5/. In addition, data used to assess the ability of the models were taken from the National Centers for Environmental Prediction–National Center for Atmospheric Research (NCEP–NCAR) reanalysis [29] of monthly meridional winds at 850 hPa and 10 m (hereafter referred to as observation).

Since the response of climate models to the same or similar forcing conditions differs from model to model, the multi-model ensemble mean with the same [30] or different [31] weights is generally used to obtain common results of climate models in the literature. In this study, multiple ensemble runs, as shown in Table 1, were first averaged into a set of data with the same weights. Second, all model and observation data were aggregated to a relatively mid-range horizontal resolution of 144 × 90 (longitude × latitude, roughly equivalent to 2.5° × 2°) through a bilinear or area-based interpolation algorithm. The ensemble mean of multiple climate models was then obtained using the same weights across the reliable models of concern. In addition, considering that climate change projection is with respect to the late-20th century, that part of the 20C3M simulations ends in the year 1999, and that the NCEP–NCAR reanalysis data are more reliable after 1979 owing to the availability of satellite data, the period 1980–1999 was chosen as the reference period here.

2 Evaluation of the models

It is widely accepted that the East Asian monsoon is composed of tropical and subtropical monsoon circulations, and that wind directions are generally opposite in the lower troposphere between winter and summer [14,15]. In winter, northeasterly winds prevail in the lower troposphere below about 700 hPa over the eastern side of the Siberian high and over coastal East Asia. These air flows are divided into two branches in the areas south of Japan. One turns eastward to the subtropical western North Pacific, and the other turns southward and flows along coastal East Asia and onto the South China Sea. Because northerly winds are most significant in the near-surface atmosphere, the geographical distribution of meridional wind at 10 m was used to evaluate the ability of the models on the basis of 124 grid points within the regions of 25°–40°N and 120°–140°E together with 10°–25°N and 110°–130°E according to previous studies [9,14,15,32]. In summer, southerly winds prevail in the lower troposphere, particularly at 850 hPa, over East China and the western side of the western North Pacific subtropical high. Referring to previous studies [14,15,33], meridional wind at 850 hPa was used to evaluate the ability of the models based on 60 grid points within the region of 20°–40°N and 105°–120°E.

To objectively measure the ability of the models to simulate the East Asian monsoon, spatial correlation coefficients (SCCs) between simulated and observed climatology of meridional wind at 10 m in winter and at 850 hPa in summer for the period 1980–1999 were calculated model by model, as well as the standard deviation and centered root mean square difference (RMSD) of each simulation with respect to observation based on the grid points within the aforementioned target regions. As shown in the Taylor diagram [34], all 36 climate models with data available (Table 1) could reliably reproduce the geographical distribution of winter meridional wind at 10 m (Figure 1(a)). SCCs ranged from 0.44 (GISS-ER) to 0.84 (IPSL-CM4 and IPSL-CM5A-

Table 1 Basic information on the 23 CMIP3 models and 19 CMIP5 models as well as their experiments

Model ID		Country	Atmospheric resolution	Integration period	Experiment and ensemble size		No data for wind at 10 m
23 climate models in the CMIP3					20C3M	A1B	
1	BCCR-BCM2.0	Norway	T42, L31	1850–2099	1	1	
2	CCSM3	USA	T85, L26	1870–2100	7	7	√
3	CGCM3.1(T47)	Canada	T47, L31	1850–2100	1	1	
4	CGCM3.1(T63)	Canada	T63, L31	1850–2100	1	1	
5	CNRM-CM3	France	T42, L45	1860–2100	1	1	
6	CSIRO-Mk3.0	Australia	T63, L18	1871–2100	3	1	√
7	CSIRO-Mk3.5	Australia	T63, L18	1871–2100	3	1	
8	ECHAM5/MPI-OM	Germany	T63, L32	1860–2100	4	4	
9	FGOALS-g1.0	China	128 × 60, L9	1850–2099	3	3	
10	GFDL-CM2.0	USA	144 × 90, L24	1861–2100	3	1	
11	GFDL-CM2.1	USA	144 × 90, L24	1861–2100	3	1	
12	GISS-AOM	USA	90 × 60, L20	1850–2100	2	2	
13	GISS-EH	USA	72 × 46, L20	1880–2099	5	3	
14	GISS-ER	USA	72 × 46, L20	1880–2100	9	5	
15	INGV-SXG	Italy	T106, L19	1870–2100	1	1	√
16	INM-CM3.0	Russia	72 × 45, L21	1871–2100	1	1	
17	IPSL-CM4	France	96 × 72, L19	1860–2099	1	1	
18	MIROC3.2(hires)	Japan	T106, L56	1850–2100	1	1	
19	MIROC3.2(medres)	Japan	T42, L20	1850–2100	3	3	
20	MRI-CGCM2.3.2	Japan	T42, L30	1851–2100	5	5	
21	PCM	USA	T42, L18	1890–2099	4	3	√
22	UKMO-HadCM3	UK	96 × 73, L19	1860–2099	2	1	
23	UKMO-HadGEM1	UK	192 × 145, L38	1860–2099	2	1	
19 climate models in the CMIP5					Historical	RCP4.5	
24	BCC-CSM1.1	China	T42, L26	1850–2099	1	1	
25	CanESM2	Canada	T63, L35	1850–2100	5	5	
26	CCSM4	USA	288 × 192, L26	1850–2100	6	5	√
27	CNRM-CM5	France	256 × 128, L31	1850–2100	10	1	
28	CSIRO-Mk3.6.0	Australia	192 × 96, L18	1850–2100	1	1	
29	FGOALS-g2	China	128 × 60, L26	1850–2100	1	1	√
30	FGOALS-s2	China	128 × 108, L26	1850–2100	3	3	
31	GISS-E2-R	USA	144 × 90, L40	1850–2100	1	1	
32	HadGEM2-ES	UK	192 × 145, L38	1850–2100	4	4	
33	INM-CM4	Russia	180 × 120, L21	1850–2100	1	1	
34	IPSL-CM5A-LR	France	96 × 95, L39	1850–2100	4	4	
35	IPSL-CM5A-MR	France	144 × 143, L39	1850–2100	1	1	
36	MIROC5	Japan	T85, L40	1850–2100	3	1	
37	MIROC-ESM	Japan	T42, L80	1850–2100	3	1	
38	MIROC-ESM-CHEM	Japan	T42, L80	1850–2100	1	1	
39	MPI-ESM-LR	Germany	T63, L47	1850–2100	3	3	
40	MRI-CGCM3	Japan	320 × 160, L48	1850–2100	3	1	
41	NorESM1-M	Norway	144 × 96, L26	1850–2100	3	1	
42	NorESM1-ME	Norway	144 × 96, L26	1850–2100	1	1	

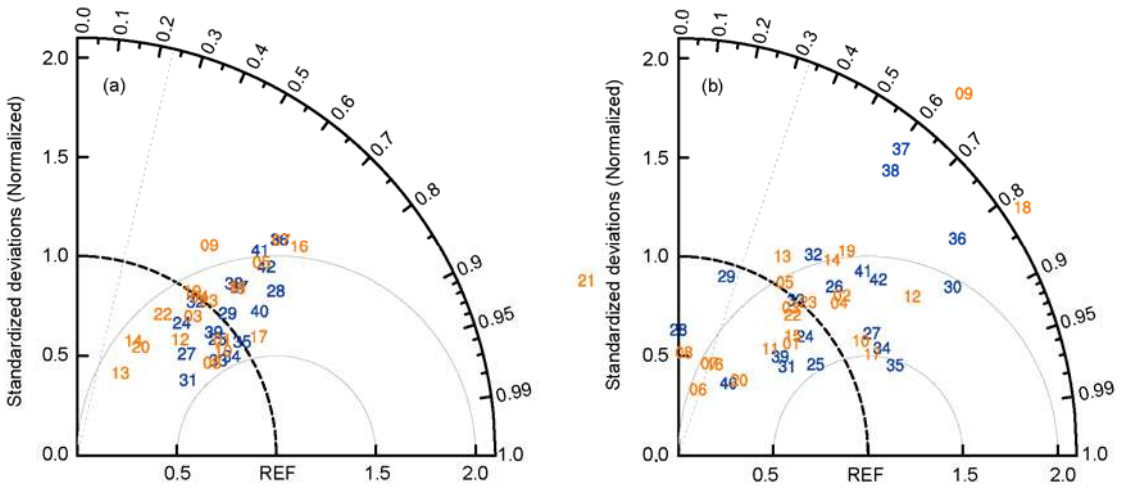

Figure 1 Taylor diagram for displaying normalized pattern statistics of climatological meridional wind (a) at 10 m within the regions of 25°–40°N and 120°–140°E together with 10°–25°N and 110°–130°E between the 36 climate models and observation in winter, and (b) at 850 hPa within the region of 20°–40°N and 105°–120°E between the 42 climate models and observation in summer for the reference period 1980–1999. Each number represents a Model ID (see Table 1); orange and blue represent the CMIP3 and CMIP5 models, respectively; and observation is considered as the reference (REF). Standard deviation and centered root mean square difference are normalized by the reference standard deviation. The radial distance from the origin is the normalized standard deviation of a model; the correlation between a model and the reference is given by the azimuthal position of the model, with oblique dotted line showing the 99% confidence level; and the centered root mean square difference between a model and the reference is their distance apart. In brief, the nearer the distance between a number and REF, the better the performance of the corresponding model.

LR), and all of them were statistically significant at the 99% confidence level. Normalized centered RMSDs ranged from 0.55 (IPSL-CM5A-LR) to 1.12 (FGOALS-g1.0), with the values of CSIRO-Mk3.5, FGOALS-g1.0, INM-CM3.0, MIROC5, and NorESM1-M being more than 1.00 and those of all the other 31 models being within 0.50–1.00. In summer, there was a large spread in the ability of 42 climate models to represent the present meridional wind at 850 hPa (Figure 1(b)). SCCs ranged from –0.49 (PCM) to 0.93 (IPSL-CM5A-MR), and the values of CSIRO-Mk3.0, ECHAM5/MPI-OM, PCM, CSIRO-Mk3.6.0, and FGOALS-g2 were not statistically significant at the 99% confidence level. Normalized centered RMSDs ranged from 0.47 (IPSL-CM5A-MR) to 1.85 (FGOALS-g1.0), with the values of 12 models being more than 1.00. Collectively, the ability of the models to simulate the EAWM was found to be reliable and relatively concentrated, with an overall better performance for the CMIP5 models compared to the CMIP3 models, and the ability to simulate the EASM was found to be relatively weak and dispersed, with a comparable performance between the CMIP3 and CMIP5 models. Thus, it was necessary to exclude those unreliable models from the present study. As such, two preconditions were arbitrarily set to identify reliable models for both the EAWM and EASM. First, SCCs had to be positive and statistically significant at the 99% confidence level; and second, normalized centered RMSDs had to be less than 1.00. In this manner, 31 (29) models, namely 16 CMIP3 plus 15 (13) CMIP5 models, were applied to investigate the EAWM (EASM) (Figure 1). Accordingly, the ensemble mean of the CMIP3 and CMIP5 models was respectively calculated using the results of 16 CMIP3 and 15 (13) CMIP5 models in winter (summer).

3 Results

There have been more than twenty indices of the East Asian monsoon intensity published in the literature. Considering that there are complex relationships between the present East Asian monsoon and other climate variables, and that we do not know whether those relationships are still valid under future global warming, it should be more reasonable to gauge the strength of the East Asian monsoon directly through wind speeds rather than indirectly through other variables. In this context, regionally averaged meridional wind at 10 m within the regions of 25°–40°N and 120°–140°E together with 10°–25°N and 110°–130°E was used to measure the EAWM intensity according to previous work [32], and regionally averaged meridional wind at 850 hPa within the region of 20°–40°N and 105°–120°E was used to measure the EASM intensity. To reduce the influence of the differences in the East Asian monsoon climatology among the models and their ensemble means, the percentage change of those intensity values relative to the 1980–1999 climatology was chosen as the EAWM or EASM intensity index (hereafter referred to as MW-index) for each model and their ensemble mean. Note that meridional winds have been widely used to gauge the East Asian monsoon intensity previously [9,33,35]. Furthermore, another widely used index of the strength of the East Asian monsoon (hereafter referred to as SLP-index), defined by zonal sea level pressure difference [36,37], was also calcu-

lated, so as to avoid index-dependent results. To compare indices more transparently, the original index of the EAWM intensity was revised as the percentage change relative to the climatology for the reference period 1980–1999.

3.1 Projection of the EAWM

Figure 2 shows that the EAWM intensity varies slightly over the 21st century relative to 1980–1999 based on the results of either individual models or their ensemble means and of either the MW-index or SLP-index. In detail, the MW-index decreases (increases) in 19 (12) out of the 31 models and decreases in the CMIP3, CMIP5, and 31-model ensemble means over the whole period 2000–2099. However, most of those changes are small. Statistically significant decreased (increased) trends at the 95% confidence level can be identified in only five models and the CMIP3 and 31-model ensemble means (two models). On the other hand, the SLP-index decreases (increases) in 15 (16) out of the 31 models, and it decreases in the CMIP3 model ensemble mean but increases in the CMIP5 and 31-model ensemble means. Statistically significant decreased (increased) trends can be identified in only five models (six models and the CMIP5 model ensemble mean). Both the MW-index and SLP-index trends are statistically significantly negative in GISS-EH, GISS-ER, and CSIRO-Mk3.6.0 but positive in IPSL-CM5A-MR. Taken together, future changes in the EAWM intensity are model and index dependent, implying that the previous conclusion on the EAWM weakening drawn from individual or several models [7,16,24,25] is uncertain. On the whole, there is no significant change trend for the EAWM in the 21st century based on the present 31 climate models.

At the regional scale, the EAWM weakens (strengthens) north (south) of about 25°N in East Asia over the 21st century. This can be explained by the following dynamical mechanism. During 2080–2099, for example, the Aleutian Low weakens and moves northward relative to the reference

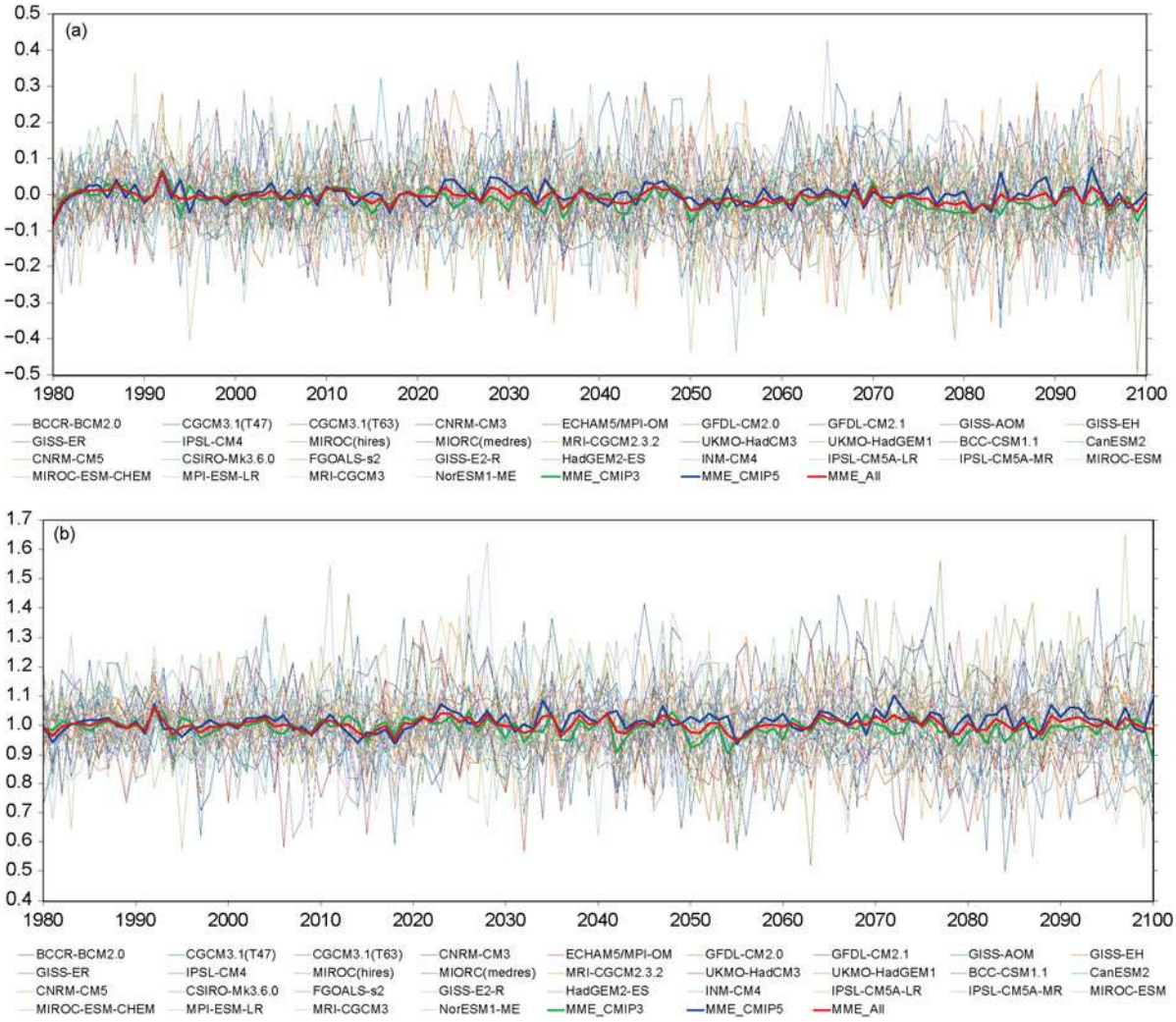

Figure 2 East Asian winter monsoon intensity indices as measured by meridional wind at 10 m (a) and zonal sea level pressure difference (b), in which MME_CMIP3, MME_CMIP5, and MME_All denote the ensemble mean of the 16 CMIP3 models, 15 CMIP5 models, and all the 31 models, respectively.

period 1980–1999 based on the 31-model ensemble mean (Figure 3), which is consistent with previous results [24]. Accordingly, an anomalous anticyclonic circulation occurs over the mid-high latitudes of the North Pacific. It leads to a weakening of climatological northerly winds over Northeast Asia. On the other hand, temperature increase is larger over the mid-high latitudes of eastern Eurasia than over the western North Pacific as a consequence of the difference in heat capacity between land and ocean. As a result, northwest–southeast thermal and sea level pressure differences decrease across Northeast Asia (Figure 4(a)), and in turn northwesterly winds weaken there. Both processes determine the EAWM weakening north of about 25°N in East Asia (Figure 3(b)). For the reference period 1980–1999, climatological northerly winds at 10 m within the region of 10°–25°N and 110°–130°E come from coastal air flows from the north and northeasterly air flows from the low latitudes of the western North Pacific, with the latter being dominant (Figure 3(a)). As shown in Figure 3(b), in response to the weakening and northward shift of the Aleutian Low, the southern branch of the aforementioned large-scale anomalous anticyclonic circulation over the mid-high latitudes of the North Pacific are anomalous easterly winds. They strengthen climatological northeasterly winds over the low latitudes of the western North Pacific, and in turn northerly winds strengthen south of about 25°N in East Asia.

Winter monsoon has been projected to weaken or slightly weaken over East China in previous studies based on individual models [7,16,25] and multiple models without a necessary quality control [17,24]. Figure 3(b) clearly shows that there are no large-scale atmospheric circulation anomalies in East China, apart from in Northeast China where anomalous westerly winds strengthen climatological northwesterly winds. This agrees generally with the previous results of 18 CMIP3 models under the SRES A1B scenario [22].

3.2 Projection of the EASM

Figure 5 shows that there is no significant change trend for the intensity of the EASM over the 21st century as a whole, and it is only slightly strengthened and features a slightly increased interannual variability relative to the reference period. The MW-index increases (decreases) in 19 (10) out of the 29 models over the whole period 2000–2099, six (two) of which are statistically significant at the 95% confidence level. It slightly increases in the 29-model ensemble mean

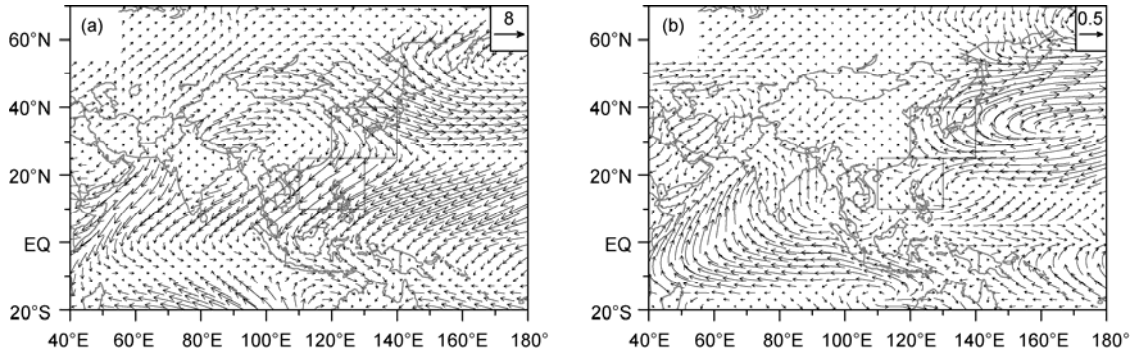

Figure 3 (a) Climatology of winter wind at 10 m for 1980–1999; (b) the corresponding difference between the periods 2080–2099 and 1980–1999 from the 31-model ensemble mean (units: m s^{-1}). Two rectangles show the regions of 25°–40°N and 120°–140°E, and 10°–25°N and 110°–130°E.

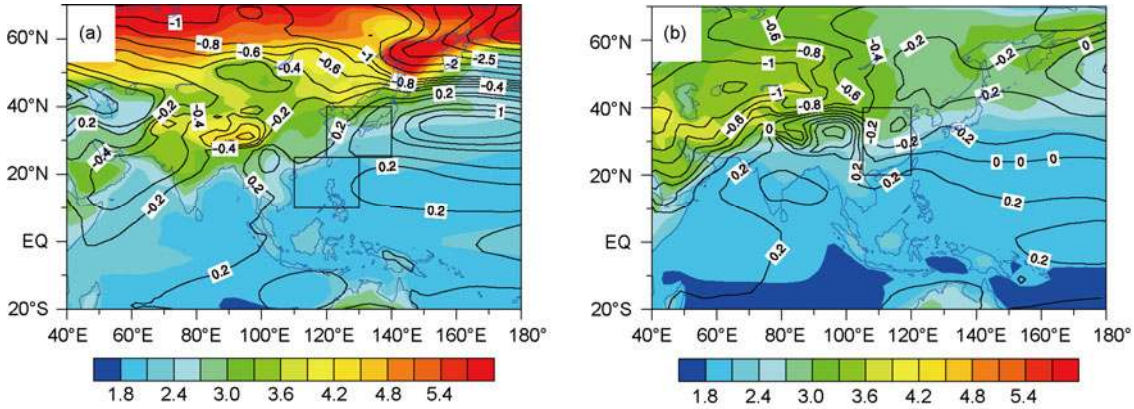

Figure 4 (a) Changes in winter temperature (shading; units: K) and sea level pressure (contour; units: hPa) between the periods 2080–2099 and 1980–1999 as derived from the 31-model ensemble mean, and two rectangles show the same regions as in Figure 3. (b) Same as in (a), but for summer from the 29-model ensemble mean, and rectangle showing the region of 20°–40°N and 105°–120°E.

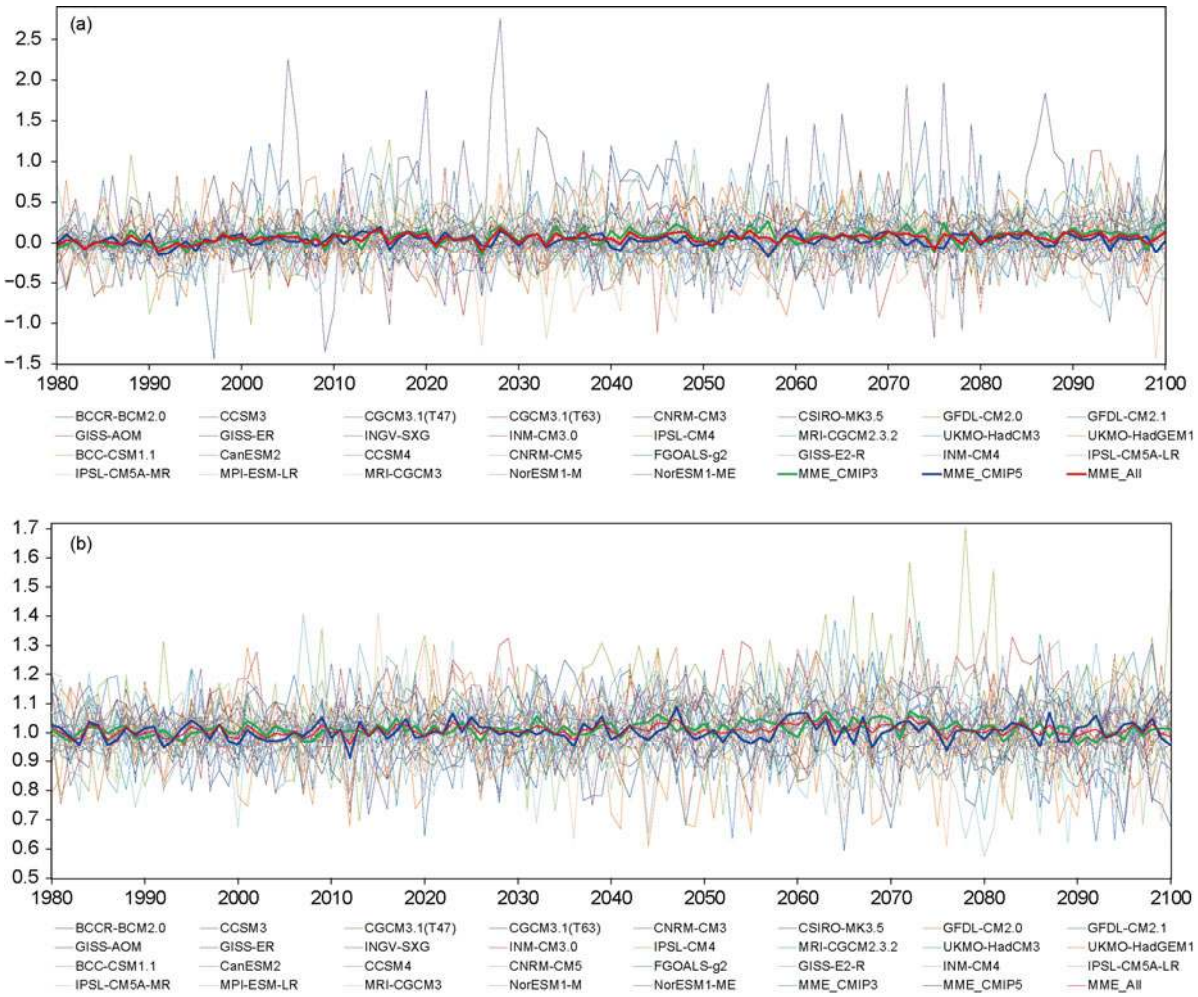

Figure 5 East Asian summer monsoon intensity indices as measured by meridional wind at 850 hPa (a) and zonal sea level pressure difference (b), in which MME_CMIP3, MME_CMIP5, and MME_All denote the ensemble mean of the 16 CMIP3 models, 13 CMIP5 models, and all the 29 models, respectively.

with a non-significant trend. Similarly, the SLP-index increases in 16 (13) out of the 29 models, six (four) of which are statistically significant. There is a non-significant increased trend for the 29-model ensemble mean. Both the MW-index and SLP-index trends are statistically significantly positive in CCSM3, GISS-ER, UKMO-HadCM3, and FGOALS-g2 but negative in MPI-ESM-LR. In this situation, future changes in the EAWM intensity are also model and index dependent, as is the case for winter. On the whole, the EASM intensity is slightly strengthened over the 21st century based on the ensemble result of either individual models or the models with statistically significant trends. Such a slight strengthening is consistent in direction with most of the previous studies [5,7,16–19] but disagrees with the previous results of little change [22] and normal intensity [23]. In addition, it is noted that the standard deviation of the MW-index and SLP-index series as derived from the 29-model ensemble mean increases by 2.3% and 4.7% for 2000–2099 relative to the reference period, respectively. That means the interannual variability of the EASM intensity increases over the 21st century, which is in line with the increased interannual variability of the EASM rainfall under future global warming as revealed by 12 CMIP3 models [38].

The above slight strengthening of the EASM over the 21st century is further confirmed by atmospheric circulation changes in the lower troposphere, as large-scale southerly wind anomalies (less than 1 m s^{-1}) at 850 hPa prevail over East and Northeast China in the 29-model ensemble mean for 2080–2099 relative to the reference period (Figure 6). This is because under future global warming, temperature rises across East Asia and adjacent areas but with a different magnitude between land and ocean (Figure 4(b)). On the one hand, the rate of warming is faster over East Asia than over the same latitudes of the western North Pacific and hence leads to an increased zonal thermal contrast. Accordingly, the strengthening of heat low over the East Asian continent is larger in magnitude than the weakening of the western North Pacific subtropical high, leading to an increased zonal sea level pressure gradient and in turn southerly wind

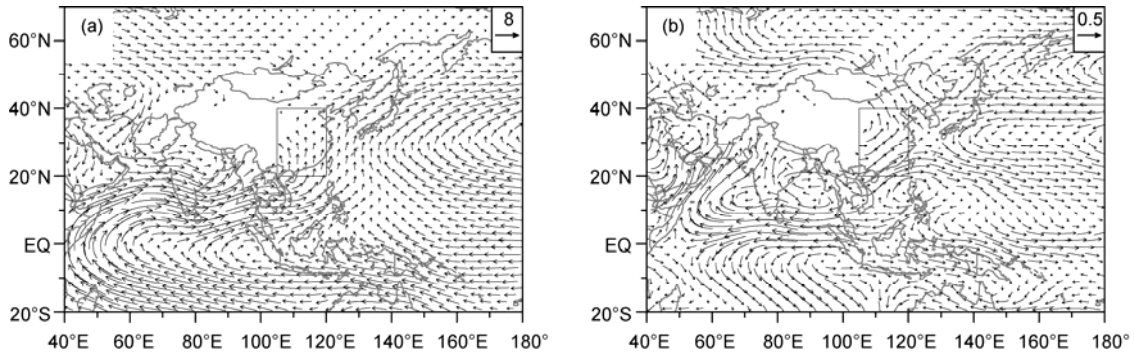

Figure 6 (a) Climatology of summer wind at 850 hPa for 1980–1999; (b) the corresponding difference between the periods 2080–2099 and 1980–1999 from the 29-model ensemble mean (units: m s^{-1}). Regions with an elevation above 1500 m are left blank, and the rectangle shows the region of 20°–40°N and 105°–120°E.

anomalies over East Asia. On the other hand, the rate of warming is faster over East China than over the South China Sea. This leads to increased meridional land–sea thermal and sea level pressure gradients and hence southerly wind anomalies over South China. Collectively, the above changes in zonal and meridional land-sea thermal contrasts across East Asia and surrounding oceans are responsible for the slight strengthening of the EASM.

In previous work performed using the CMIP3 dataset under the SRES A1B scenario, the EASM was projected to strengthen by 23 [17] and 15 [19] models, strengthen only over South China by 8 [20] and 19 [21] models, vary little by 18 models [22], and remain normal in terms of intensity by 14 models [23]. Such discrepancies are not strange when viewed from this study, because, apart from the difference in methods and research areas, the EASM change is determined largely by climate models used in analysis. In other words, those projections are more or less model dependent, owing to a limited number of climate models. Using all data of 29 reliable climate models, particularly those of 13 CMIP5 models under the latest RCP4.5 scenario, the slight strengthening of the EASM, as well as the underlying mechanisms, over the 21st century drawn from the present study should be relatively objective.

4 Discussion and conclusion

In recent years, many climate models have been used to project future climate change worldwide. Under the most representative SRES A1B or RCP4.5 scenario, this study assessed the East Asian winter and summer monsoon changes over the 21st century using the data of 31 and 29 reliable climate models, respectively. Those models were selected from all available 42 climate models participating in the IPCC Assessment Reports Four and Five in terms of their ability to simulate the present East Asian monsoon climatology. Under future global warming, it was found there is no significant trend for the EAWM intensity as a whole. At the regional scale, the EAWM weakens (strengthens) north (south) of about 25°N in East Asia as a consequence of the weakening and northward shift of the Aleutian Low and of decreased northwest–southeast thermal contrasts across Northeast Asia. In summer, monsoon strengthens slightly in East China because of increased zonal and meridional land-sea thermal contrasts over the 21st century.

It was also noted that the future East Asian monsoon changes are somewhat model and index dependent. This explains why there are discrepancies on this issue in previous studies, and implies that more emphasis should be given to the ensemble mean of multiple reliable climate models and the accompanying mechanisms. In addition, the horizontal resolution of state-of-the-art climate models is generally higher than before, along with a slightly improved simulation of the EAWM climatology. However, their ability to represent the East Asian climate is still inadequate, and hence their projection is more or less uncertain. Given that the performance of high resolution regional climate models to simulate the present climate over China is better overall than that of global climate models [39–41], and that future changes in monsoon precipitation over China are different between regional and global models [41], more attention should be paid to dynamical downscaling studies at the regional scale. Finally, we would like to emphasize that there are uncertainties in future emissions or concentration scenarios of greenhouse gases and aerosols, or in radiative forcing scenarios. There are still incomplete aspects in the global climate or earth system models. The lack of observation data hampers our understanding of climate change on the decadal and longer timescales. Our knowledge of natural climate variability over a range of timescales is also limited. All these factors lead to a level of uncertainty in future climate change projection.

We sincerely thank the three anonymous reviewers for their helpful comments and suggestions on the earlier version of the manuscript. Also, we acknowledge the World Climate Research Programme's Working Group on Coupled Modelling, which is responsible for CMIP, and we thank the climate modeling groups (listed in Table 1 of this paper) for producing and

making available their model output. For CMIP the U.S. Department of Energy's Program for Climate Model Diagnosis and Intercomparison provides coordinating support and led development of software infrastructure in partnership with the Global Organization for Earth System Science Portals. This work was supported by the National Basic Research Program of China (2009CB421407) and the National Natural Science Foundation of China (41175072).

1 Wang H J. The weakening of the Asian monsoon circulation after the end of 1970's. Adv Atmos Sci, 2001, 18: 376–386
2 Xue F. Interannual to interdecadal variation of East Asian summer monsoon and its association with the global atmospheric circulation and sea surface temperature. Adv Atmos Sci, 2001, 18: 567–575
3 Wang H J. The instability of the East Asian summer monsoon–ENSO relations. Adv Atmos Sci, 2002, 19: 1–11
4 Yu R C, Wang B, Zhou T J. Tropospheric cooling and summer monsoon weakening trend over East Asia. Geophys Res Lett, 2004, 31: L22212, doi: 10.1029/2004GL021270
5 Jiang D, Wang H J. Natural interdecadal weakening of East Asian summer monsoon in the late 20th century. Chin Sci Bull, 2005, 50: 1923–1929
6 Xu M, Chang C P, Fu C B, et al. Steady decline of east Asian monsoon winds, 1969–2000: Evidence from direct ground measurements of wind speed. J Geophys Res, 2006, 111: D24111
7 Ding Y H, Ren G Y, Zhao Z C, et al. Detection, causes and projection of climate change over China: An overview of recent progress. Adv Atmos Sci, 2007, 24: 954–971
8 Ding Y H, Wang Z Y, Sun Y. Inter-decadal variation of the summer precipitation in East China and its association with decreasing Asian summer monsoon. Part I: Observed evidences. Int J Climatol, 2008, 28: 1139–1161
9 Wang L, Chen W. How well do existing indices measure the strength of the East Asian winter monsoon? Adv Atmos Sci, 2010, 27: 855–870
10 Liu H W, Zhou T J, Zhu Y X, et al. The strengthening East Asian summer monsoon since the early 1990s. Chin Sci Bull, 2012, 57: 1553–1558
11 Wang H J, He S P. Weakening relationship between East Asian winter monsoon and ENSO after mid-1970s. Chin Sci Bull, 2012, 57: 3535–3540
12 Wang H J, Zeng Q C, Zhang X H. The numerical simulation of the climatic change caused by CO_2 doubling. Sci China Ser B, 1993, 36: 451–462
13 Wang H J, Sun J Q, Chen H P, et al. Extreme climate in China: Facts, simulation and projection. Meteorol Z, 2012, 21: 279–304
14 Tao S Y, Chen L X. A review of recent research on the East Asian monsoon in China. In: Chang C P, Krishnamurti T N, eds. Monsoon Meteorology. Oxford: Oxford University Press, 1987. 60–92
15 Ding Y H. Monsoons over China. Heidelberg: Springer, 1994. 1–419
16 Bueh C. Simulation of the future change of East Asian monsoon climate using the IPCC SRES A2 and B2 scenarios. Chin Sci Bull, 2003, 48: 1024–1030
17 Li B, Zhou T J. Projected climate change over China under SRES A1B scenario: Multi-model ensemble and uncertainties (in Chinese). Adv Clim Change Res, 2010, 6: 270–276
18 Sun Y, Ding Y H. Responses of South and East Asian summer monsoons to different land-sea temperature increases under a warming scenario. Chin Sci Bull, 2011, 56: 2718–2726
19 Chen H P, Sun J Q, Chen X L. The projection and uncertainty analysis of summer precipitation in China and the variations of associated atmospheric circulation field (in Chinese). Clim Environ Res, 2012, 17: 171–183
20 Ueda H, Iwai A, Kuwako K, et al. Impact of anthropogenic forcing on the Asian summer monsoon as simulated by eight GCMs. Geophys Res Lett, 2006, 33: L06703
21 Sun Y, Ding Y H. A projection of future changes in summer precipitation and monsoon in East Asia. Sci China-Earth Sci, 2010, 53: 284–300
22 Kimoto M. Simulated change of the east Asian circulation under global warming scenario. Geophys Res Lett, 2005, 32: L16701
23 Li J, Wu Z, Jiang Z, et al. Can global warming strengthen the East Asian summer monsoon? J Clim, 2010, 23: 6696–6705
24 Hori M E, Ueda H. Impact of global warming on the East Asian winter monsoon as revealed by nine coupled atmosphere-ocean GCMs. Geophys Res Lett, 2006, 33: L03713
25 Hu Z, Bengtsson L, Arpe K. Impact of global warming on the Asian winter monsoon in a coupled GCM. J Geophys Res, 2000, 105: 4607–4624
26 Nakicenovic N, Swart R. Special Report on Emissions Scenarios, A special report of Working Group III of the Intergovernmental Panel on Climate Change. Cambridge: Cambridge University Press, 2000. 1–599
27 Moss R H, Edmonds J A, Hibbard K A, et al. The next generation of scenarios for climate change research and assessment. Nature, 2010, 463: 747–756
28 Thomson A M, Calvin K V, Smith S J, et al. RCP4.5: A pathway for stabilization of radiative forcing by 2100. Clim Change, 2011, 109: 77–94
29 Kalnay E, Kanamitsu M, Kistler R, et al. The NCEP/NCAR Reanalysis Project. Bull Amer Meteorol Soc, 1996, 77: 437–472
30 Meehl G A, Stocker T F, Collins W D, et al. Global Climate Projections. In: Solomon S, Qin D, Manning M, et al., eds. Climate Change 2007: The Physical Science Basis. Contribution of Working Group I to the Fourth Assessment Report of the Intergovernmental Panel on Climate Change. Cambridge, United Kingdom and New York: Cambridge University Press, 2007. 748–845
31 Xu Y, Gao X J, Giorgi F. Upgrades to the reliability ensemble averaging method for producing probabilistic climate-change projections. Clim Res, 2010, 41: 61–81
32 Chen W, Graf H, Huang R. The interannual variability of East Asian winter monsoon and its relation to the summer monsoon. Adv Atmos Sci, 2000, 17: 48–60
33 Wang B, Wu Z, Li J, et al. How to measure the strength of the East Asian summer monsoon. J Clim, 2008, 21: 4449–4463
34 Taylor K E. Summarizing multiple aspects of model performance in a single diagram. J Geophys Res, 2001, 106: 7183–7192
35 Jiang D, Lang X. Last Glacial Maximum East Asian monsoon: Results of PMIP simulations. J Clim, 2010, 23: 5030–5038
36 Guo Q Y. Relationship between the variations of East Asian winter monsoon and temperature anomalies in China (in Chinese). Quart J Appl Meteorol, 1994, 5: 218–225
37 Guo Q Y, Cai J N, Shao X M, et al. Interdecadal variability of East–Asian summer monsoon and its impact on the climate of China (in Chinese). Acta Geogr Sin, 2003, 58: 569–576
38 Lu R Y, Fu Y H. Intensification of East Asian summer rainfall interannual variability in the twenty-first century simulated by 12 CMIP3 coupled models. J Clim, 2010, 23: 3316–3331
39 Zhang D F, Gao X J, Ouyang L C. Simulation of present climate over East Asia by a regional climate model. J Trop Meteorol, 2008, 14: 19–23
40 Yu E T, Wang H J, Sun J Q. A quick report on a dynamical downscaling simulation over China using the nested model. Atmos Oceanic Sci Lett, 2010, 3: 325–329
41 Gao X J, Shi Y, Zhang D F, et al. Uncertainties in monsoon precipitation projections over China: Results from two high-resolution RCM simulations. Clim Res, 2012, 52: 213–226